Supplementary Material (ESI) for Chemical Communications

Direct Observation and pH Control of Reversed Supramolecular Chirality in Insulin Fibrils by Vibrational Circular Dichrosim

Dmitry Kurouski,[b] Rosina A. Lombardi,[a] Rina K. Dukor,[c] Igor K. Lednev[b]* and Laurence A. Nafie[a,c]*

[a]*Department of Chemistry, Syracuse University, Syracuse, New York, 13244*

[b]*Department of Chemistry, University at Albany, SUNY, Albany, New York, 12222*

[c]*BioTools, Inc., 17546 Bee Line Hwy, Jupiter, Florida, 33458*

RECEIVED DATE (automatically inserted by publisher); E-mail: lnafie@syr.edu, lednev@albany.edu

Supporting Information

1. FTIR absorbance spectra to accompany Fig. 1. This figure demonstrates that the absorbance levels of the FT-IR spectra of the film samples were reduced from those of the solutions samples by approximately a factor 2 and this correlates with the VCD intensities of the film being reduced relative to those of the solution samples by approximately the same factor. All solution-state IR and VCD spectra in Figs. 1, 2, S1 and S2 were measured using a 6-micron pathlength BioCell (BioTools, Inc. Jupiter, FL) with etched and polished CaF_2 windows requiring no spacer. Corresponding fibril films were prepared by placing a few drops of solution on a standard CaF_2 window and allowing the sample to dry before IR and VCD measurement.

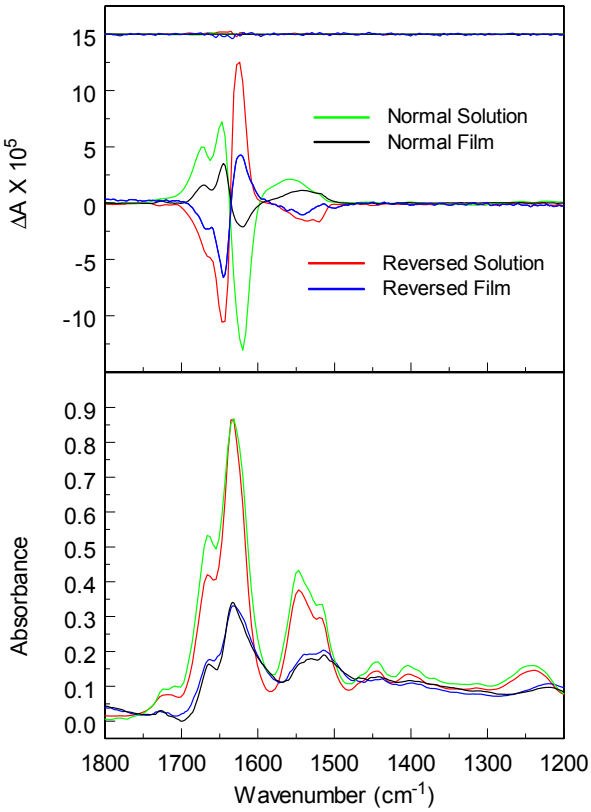

Figure S1. VCD spectra with associated IR spectra corresponding to Fig. 1. The top spectral traces represent the VCD noise levels. The middle curves are VCD spectra of normal and reversed fibril solutions and films, and the bottom spectra are the corresponding IR spectra with the same color designations.

2. Composite figure combining the VCD spectra presented in Fig 2. This figure shows all pH controlled VCD spectra measured.

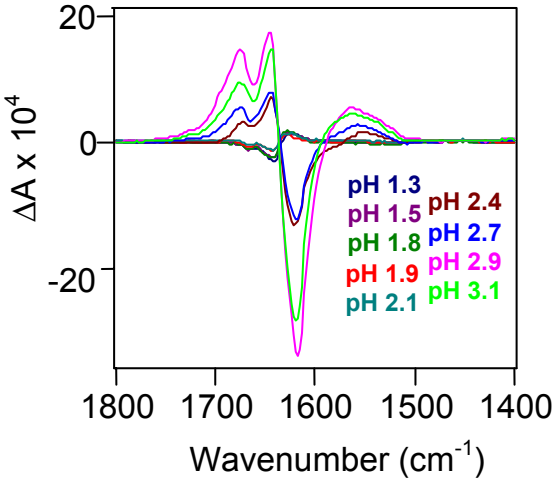

Figure S2. Composite of all nine VCD spectra at pH values 3.1, 2.9, 2.7, 2.4, 2.1, 1.9, 1.8, 1.5 and 1.3 shows the relative intensities of the normal and reversed fibril VCD spectra. The VCD spectra of the reversed fibrils at low pH are noisier than those of normal fibrils at high pH because the former were measured at IR absorbances between 0.1 and 0.2 at the peak of the amide I band whereas the latter were measured with amide I peak absorbance values near 0.8. We found no difference in solubility between normal and reversed fibrils in aqueous solution. All IR and VCD were then scaled by to a peak amide I band absorbance of 1.0 as shown in Fig. 2 of the main document.

3. DUVRR and Preservation of Secondary Structure. Since amyloid fibrils are noncrystalline and insoluble, the application of classical tools of structural biology, namely X-ray crystallography and solution NMR, is limited. However, wide-angle X-ray scattering from flow-oriented fibrils has been utilized to estimate interstrand and intersheet spacing of cross-β-structures.[1] Solid-state NMR probes interatomic distances and torsion angles, which define local secondary structure and side-chain conformations. This technique, however, requires site-specific ^{13}C and/or ^{15}N labels.[2] Further, FTIR combined with proteolysis has been used to characterize the core structure of lysozyme fibrils.[3] DUVRR spectroscopy has proven to be an efficient technique for characterizing protein structural rearrangements at all stages of fibrillation.[4-9] In particular, DUVRR spectroscopy combined with hydrogen-deuterium exchange has been utilized for characterizing the structure of the fibril core.[6] DUVRR spectroscopy is utilized here to identify the protein secondary structures of the various fibril polymorphs.

A typical protein DUVRR spectrum is dominated by amide bands, which characterize the polypeptide backbone conformation and aromatic amino acid bands by reporting on their local environment.[4] The spectra of all fibril polymorphs show sharp and intense Amide I and II bands as well as a dramatic increase of the C_α-H bending Raman cross-section. These changes indicate that the protein α-helix melts during insulin incubation under denaturating conditions and forms a cross-β-sheet fibril structure. A strong narrow Amide I DUVRR band is indicative of an extended β-sheet conformation evident for all fibril spectra in Fig. S3.

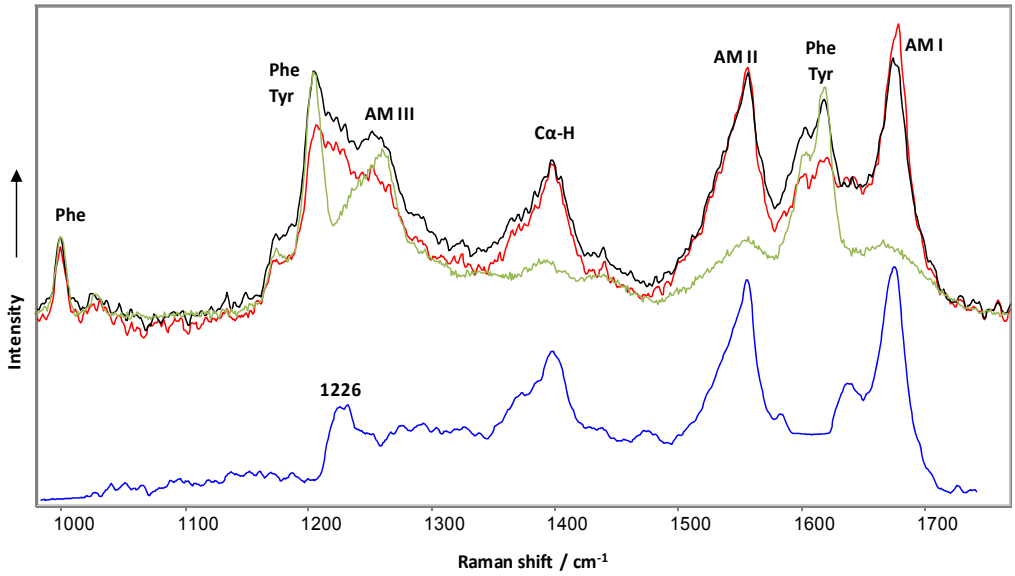

Figure S3. DUVRR spectra of insulin fibrils grown at pH 3.1 (black), 1.5 (red), native insulin (green) and the spectrum of fibril cross-β-core (blue). Amide I vibrational mode (Am I) is dominated by C=O stretching, with a small contribution from C—N stretching and N—H bending. Amide II and Amide III bands involve significant C—N stretching, N—H bending, and C—C stretching. The C_α-H bending vibration mode involves C_α-H symmetric bending and C—C_α stretching.

Hydrogen-deuterium exchange combined with DUVRR spectroscopy characterizes the secondary structure of the fibril core. The Amide III vibrational mode involving significant C–N stretching, N–H bending, and C–C stretching is the most sensitive part of DUVRR spectrum to the protein backbone conformation. According to Asher and coworkers[10], the position of Amide III_3 band reports on the Ψ dihedral angle. We found that all fibril polymorphs have the same Amide III_3 band position, representing a single peak centered at 1226 cm^{-1}. We have recently reported on lysozyme fibrils,[6] which exhibit cross-β core Raman signature with Amide III_3 band at 1226 cm^{-1} (Fig. S3, blue), that, according to Asher's semiempirical approach,[10] corresponds to β-sheet conformation characterized by Ψ dihedral angle of 135°. The fact that Ψ dihedral angle estimated from Raman spectra is the same for all insulin fibril polymorphs described in this study is significant and indicates an unchanged β-sheet conformation because this angle could be as large as 150° for other fibrils.[9] The results obtained here indicate that all fibril polymorphs, despite previously demonstrated differences in morphology and chiral fibril structure, share the same cross-β-core structure.

4. Experimental and Instrumentation Details

Insulin Fibril Preparation:

1. Dissolve ~60 mg of insulin in 1 mL water.
2. Measure pH and lower to pH 2 (the insulin will not dissolve completely until the pH is lowered).
3. Samples for Fig. 1 were heated for approximately 2h at 65 °C in an oil bath until the solution became cloudy and visibly gel-like.
4. Samples for the pH studies in Fig. 2 were prepared by heating for 24h at 70° C.

Vibrational Circular Dichroism:

VCD and IR spectra were measured at Syracuse University using a dual-source, dual-PEM Chiral*IR* Fourier transform VCD spectrometer (BioTools, Inc., Jupiter Florida) equipped with a HgCdTe detector with spectral coverage from 800 to 2000 cm^{-1}. Fibril solution samples were placed between CaF_2 windows with a pathlength of~ 6 microns in a BioCell (BioTools, Inc., Jupiter Florida) and measured at a spectral resolution of 8 cm^{-1}

Atomic Force Microscopy:

Redispersed fibrils were diluted with aqueous pH 2.0 HCl solution in a 1:800 ratio and deposited onto freshly-cleaved mica. The deposited samples were quickly dried under a nitrogen flow. AFM imaging was performed by using a MFP-3D™ Bio Asylum Research microscope (Asylum Research, CA, USA) in non-contact mode with Olympus AC160TS tips.

Deep Ultraviolet Raman Scattering:

DUVRR spectra were obtained at the University of Albany using a home-built Raman spectrometer as described elsewhere[11] with 197-nm excitation wavelength. A spinning NMR tube with a magnetic stirrer inside was used for sampling. In hydrogen-deuterium exchange experiments, samples (1mL) of fibrils dispersed in water were centrifuged at 14 000 g for 30 min. The precipitate was washed with D_2O. This procedure was performed several times. D_2O-based samples were incubated for 3h at 25˚C prior to recording to ensure significant hydrogen-deuterium exchange. Obtained dispersion in D_2O was used for Raman spectroscopic measurement. Native insulin was measured in water. All reported Raman spectra are an average of at least three independent measurements. GRAMS/AI 7.0 (Thermo Galactic, Salem, NH) was used for spectral data processing.

1. A. M. Squires, G. L. Devlin, S. L. Gras, A. K. Tickler, C. E. MacPhee and C. M. Dobson, *J. Am. Chem. Soc.,* 2006**, 128, (36)**, 11738-9.
2. R. Tycko, *Q. Rev. Biophys,* 2006**, 39, (1)**, 1-55.
3. E. Frare, M. F. Mossuto, P. Polverino de Laureto, M. Dumoulin, C. M Dobson. A. Fontana, *J. Mol. Biol.,* 2006**, 361**, **(3)**, 551-61.
4. I. K. Lednev, in Protein Structures, Methods in Protein Structures and Stability Analysis, eds. V. N. Uversky and E. A. Permyakov, Nova Sci., 2007; pp.1-26.
5. C. Arnaud, in Chem. & Eng. News, 2009, 87 (24), 10-14.
6. M. Xu, V. Shashilov and I. K. Lednev, J. Am. Chem. Soc., 2007, 129, 11002-11003.
7. V. Shashilov, M. Xu, V. V. Ermolenkov, L. Fredriksen and I. K. Lednev, J. Am. Chem. Soc., 2007, 129, 6972-6973.
8. V. A. Shashilov and I. K. Lednev, J. Am. Chem. Soc., 2008, 130, 309-317.
9. V. Sikirzhytski, N. I. Topilina, S. Higashiya, J. T. Welch and I. K. Lednev, J. Am. Chem. Soc., 2008, 130, 5852-5853.
10. A. V. Mikhonin, S. V. Bykov, N. S. Myshakina and S. A. Asher, J. Phys. Chem., 2006, 110, 1928-1943.
11. I. K. Lednev, V. V. Ermolenkov, W. He, M. Xu, *Anal. Bioanal. Chem.,* 2005**, 381, (2)**, 431-7.